ICWE14
June 21-26, 2015 | Porto Alegre - Brazil
14th INTERNATIONAL CONFERENCE ON WIND ENGINEERING

Reviewing the art of modeling 3D aeroelastic behavior of cable-stayed bridges

Ronaldo Battista[1,2], Michèle Pfeil[2], Arthur Curi[1,2], Carolina Santos[1,2],
Acir Loredo-Souza[3], Marcelo Rocha[3], Mario Klaus Oliveira[4], Maria Cristina Bênia[4], Matthew Vallis[3], Adrian Wittwer[5]
[1] Controllato Ltda., Rio de Janeiro, Brazil
[2] COPPE Institute, Universidade Federal do Rio de Janeiro, Rio de Janeiro, Brazil
[3] Faculty of Engineering, Universidade Federal do Rio Grande do Sul, Porto Alegre, Brazil
[4] Vento-S Consultoria em Engenharia do Vento Ltda., Porto Alegre, Brazil
[5] Faculty of Engineering, Universidad Nacional del Nordeste, Resistencia, Argentina
email: controllato1@gmail.com; mpfeil@coc.ufrj.br; acir@ufrgs.br; mmrocha@cpgec.ufrgs.br; mariogustavo@vento-s.com

ABSTRACT: The development of an optimized structural design and the calculation of dynamic internal forces in the complete structure of a cable-stayed bridge under wind action is properly carried out with a theoretical-computational 3D aeroelastic model. The mathematical model of the applied aerodynamic forces is formulated by taking into account the aerodynamic and aeroelastic coefficients obtained through wind tunnel tests of small scale seccional models. Physical 3D aeroelastic modeling of very long cable-stayed bridges requires very large wind tunnel facilities and it is usually time and cost prohibitive. Hence for the design of these bridges the 3D theoretical – computational model offers some practical advantages. However it needs to be validated by sound correlation of numerical results with their experimental counterpart obtained from measurements on the actual structure or more easily on its 3D physical model tested in the wind tunnel where distinct wind characteristics can be well simulated. This paper explores these technical and practical aspects and focus on the validation of the 3D theoretical model against data collected from wind tunnel tests on a 3D physical model carefully constructed in a geometric scale that can fit inside ordinary small wind tunnels.

KEY WORDS: Turbulent wind forces; Cable-stayed bridges; Theoretical & Physical Models; Design implications.

1 INTRODUCTION

The development of an optimum structural design and analyses of the dynamic structural behavior and stability of modern cable-stayed bridges under the action of turbulent wind forces can only be properly performed with the aid of tridimensional (3D) physical and mathematical-numerical aeroelastic modeling.

Today´s 3D computational fluid dynamic (CFD) modeling techniques are not yet fully feasible to deal with the focused aeroelastic problems. On the other hand bidimensional (2D) CFD modeling has been applied to investigate air-flow patterns pressure distribution and vortex-shedding around bridges cross sections. Even so 2D-CFD modeling has not been substitute for sectional small scale model tests in wind tunnels.

Conversely, 3D physical and mathematical-numerical aeroelastic modeling, that one could classify as classical modeling techniques, have been continuously developed along the last decades and are still being improved, thanks to the increasing computing capacity and software facilities for structural analysis of cable-stayed bridges and also thanks to the increasing sensitivity and precision of the micro-sensors, together with the electronic hardware systems for simultaneous multichannel signal acquisition and processing which are used in the wind-tunnel tests of small scale models.

To design and fabricate either sectional or tridimensional small scale models to be tested in the wind tunnel one needs to have the main structure´s dynamic characteristics: vibration mode shapes and associated frequencies and the relevant physical modal properties, besides the appropriate damping ratios whose values can be picked up from the technical literature. To get these dynamic characteristics a primary step is to construct a 3D finite element model (FEM) of the cable-stayed bridge structure which is made on the basis of the design drawings of the structure and its foundations.

Wind tunnel tests of a physical 3D aeroelastic model yield results in terms of acceleration x time for many characteristic points and directions in the small scale structure, for various angles of wind incidence. The displacements are obtained by means of double integration of the acceleration signals and then transformed to the prototype scale. It is worthwhile to point out that digital integration of random signals may present serious drawbacks if not done carefully with appropriate numerical schemes.

Conversely the 3D aeroelastic mathematical computational modeling of the complete cable-stayed structure and its foundations seems in many aspects to be easier or at least less complex than its physical small scale counterpart. In fact this is not so because of the inherent difficulties of adequately model the wind flow characteristics (fluctuating velocities and their spatial correlation functions and realistic vertical profiles of mean velocity and of turbulence intensities) and therefore the aerodynamic forces acting on the structure produced by turbulent wind flow. These difficulties have been circumvented by data acquired from wind tunnel measurements of air flow in various angles of incidence on a topographical model of the bridge´s site.

Description of the mathematical-experimental model for the aerodynamic wind forces acting on the structural components is done with the aid of the wind flow characteristics defined by means of: a topographical model [5], together with the aerodynamic coefficients and amplitudes versus mean wind velocity responses obtained from wind tunnel tests of rigid and moving sectional models at various angles of attack in smooth and turbulent flow. Depending on the tower´s vibration characteristics and cross section geometry, only tests on the sectional model of the bridge deck are required.

In short one may state that the art of modeling either physical or mathematical-computational 3D aeroelastic models is the art of bringing together sounding theoretical and experimental models to properly describe the dynamic structural behavior of modern cable-stayed bridges under the action of smooth and turbulent wind forces.

One also may argue that the 3D aeroelastic mathematical –computational model being less complex and time-consuming presents several practical advantages in relation to the 3D aeroelastic physical model. Among these one may cite:

(i) a 3D FEM model of the structure and its foundations is of primary concern to elaborate any of the two types of 3D aeroelastic modeling;

(ii) preliminary analysis of the aeroelastic behavior may be performed during the design stage, For that it is needed usual recommendation taken from the technical literature and parameters prescribed by design codes, apart from the aerodynamic coefficients obtained from wind tunnel tests of a sectional model of the bridge deck;

(iii) structural alterations (stiffness and mass distribution, towers height, stay-cable arrangement, etc.) can be made during early stages of the structural design;

(iv) small modifications of the deck appendages (barriers, fences etc,) and the presence of long and tall vehicles may be easily and quickly made in the sectional model, and their influences may be investigated by performing new wind tunnel tests which will give updated aerodynamic coefficients to be used in the mathematical model of the wind forces;

(v) complementary analysis of the aeroelastic behavior may be performed at the final stages of the structural design, taking into account the altered and optimized structural system;

(vi) if eventually needed a dynamic control system may be envisaged and implemented in the 3D computational model and its performance evaluated through the amplitudes of the aeroelastic responses in terms of displacements and inner forces and stress in the structure´s components including the stay-cables and their anchorages;

(vii) usual damping ratios which have been measured in main structural components of existing cable-stayed bridges and used in the structure´s design are very difficult to be reproduced in small scale 3D physical model. On the contrary they are very easily taken into account in the theoretical model, allowing for performing parametric and sensitivity analysis of the aeroelastic responses of the bridge structure;

(viii) as the last but not the least practical advantage is the overall structural analysis that can be performed with the theoretical model, which allows for calculations of displacements and internal forces in any section of any structural component.

However, one may argue that in order to benefit from the mentioned practical advantages the 3D aeroelastic mathematical-computational model has to be validated by means of correlation between the obtained theoretical and the corresponding experimental results; the latter referred to measurements made in existing cable-stayed bridges or more easily in small scale 3D aeroelastic models of these bridges, for which wind tunnel tests can be performed under controlled wind flow characteristics representative of the bridge´s site.

Validation of the previously described 3D aeroelastic mathematical-computational modeling of a cable-stayed bridge structure and its foundations is the primary concern of the present paper. This is done herein by investigating the aeroelastic behavior and by correlating the theoretical amplitudes of accelerations at characteristic points and directions with their experimental counterpart obtained from wind tunnel tests on the physical small scale 3D aeroelastic model designed and constructed to fit inside ordinary size wind tunnel facilities.

2 DESCRIPTION OF THE THEORETICAL MODEL

Short descriptions of the main steps to the theoretical 3D aeroelastic modeling are given in the following for the cable-stayed bridge taken as a case-example.

2.1 Main structural characteristics of the cable-stayed bridge

Figure 1 shows elevation and plan views of the bridge example, while Figure 2 shows its cross-section. The superstructure scheme is a three continuous spans deck with smooth curvatures both in plan and elevation which result in a small deck superelevation. Main and lateral spans are 200m and 102m long respectively. The deck structure is composed of a 3.2m high reinforced and prestressed concrete box section coupled to side trussed cantilevers totalizing 26.2m deck width. Along the

bridge axis the stay cables are arranged in a central plan fan configuration. The prestressed concrete towers are laterally braced by pairs of stay cables anchored at the transverse girders. The towers box cross section is rectangular with variable dimensions in the lower quarter and constant dimensions along the remaining 47.50m of its total height of 66.50 meters above the deck level. Each tower foundation is composed by a rigid concrete block on top of 20 reinforced concrete piles of 2.50m diameter. The soil is characterized by the presence of thick layers of clay, the first layer of soft clay reaching 23m of depth.

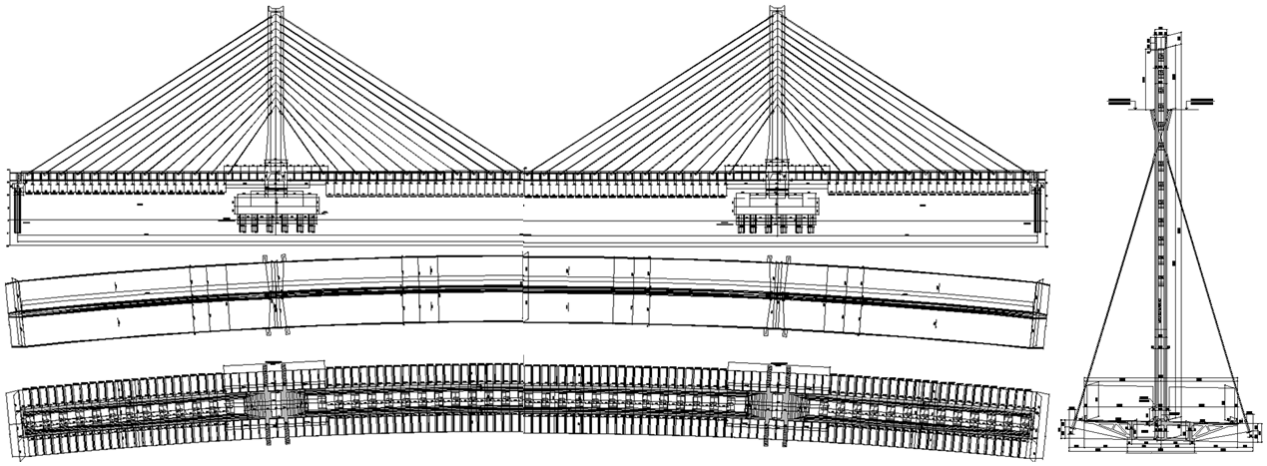

(a) (b)

Figure.1. (a) Elevation and plan views of the bridge case example; (b) Deck cross-section and tower. Designers: Enescil Engenharia de Projetos; Contractor: Consórcio Ponte de Laguna: Camargo Correa, Aterpa M.Martins; Construbase.

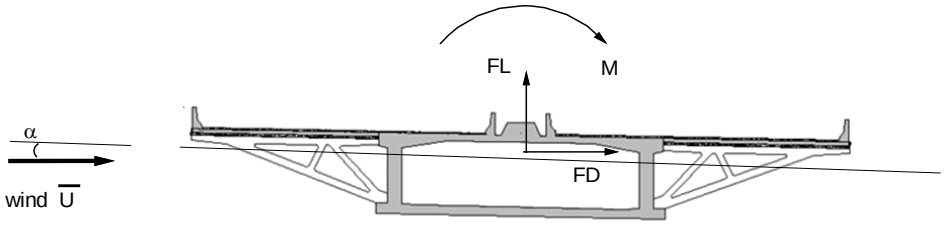

Figure.2. Deck cross-section of the bridge case example and aerodynamic force components.

2.2 Brief description of the finite element model of the structure and its foundations

Figure 3 shows the 3D finite element model of the cable-stayed bridge structure and its foundations. All the components of the superstructure are modeled with frame elements as well as the piles. The stay cables were modeled with many bar elements so as to allow adequate representation of their behavior under self- weight and prestress forces. Rigid links were provided to simulate the connections between deck and towers and deck and end supports. Also the pile cap effect is simulated by rigid links between the tower base and the top of the piles. Soil-pile interaction is considered by means of discrete spring connectors along the piles length.

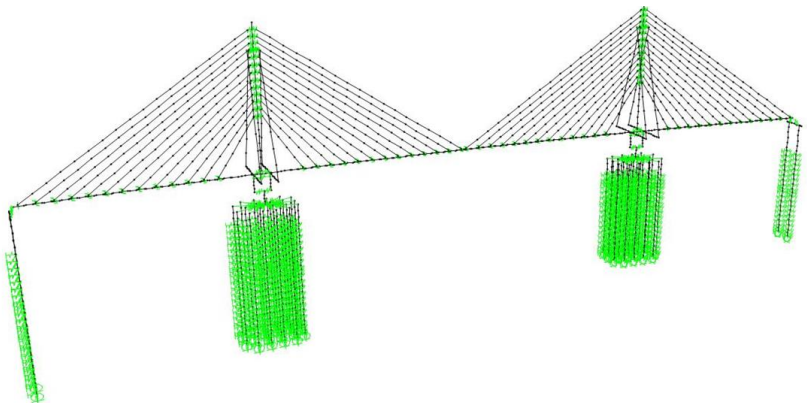

Figure.3. 3D finite element model of the bridge case example and its foundations.

2.3 Modal properties obtained from the numerical model

Free vibration analysis of the bridge structure under initial stresses produced by the prestressed stay-cables was performed to obtain its modal properties, as for example the two typical vibration mode shapes shown in Figure 4 and associated frequencies.

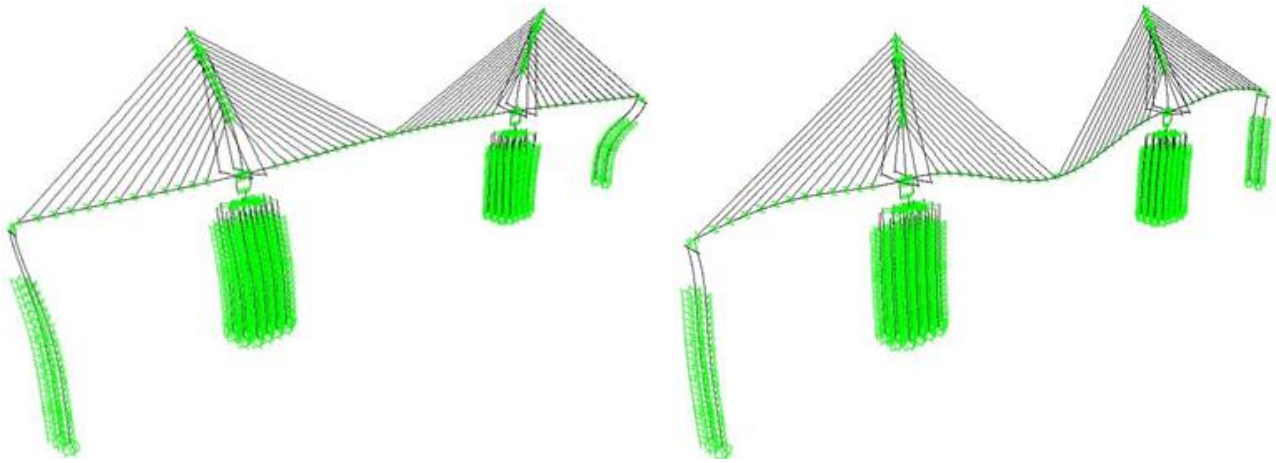

(a) (b)

Figures 4. Mode shapes; (a) dominated by lateral bending of the towers (f=0.43Hz); (b) characterized by deck vertical bending with torsion and longitudinal and lateral bending of the towers (f=0.60Hz)

2.4 Mathematical model of the aerodynamic forces

The aerodynamic forces per unit length on the bridge deck and towers (see Fig.2) are expressed in terms of three components, the drag force F_D (downwind), the lift force F_L (upward) and the torsion moment M, as a sum of static, self-excited and buffeting forces. The mean static forces are written as

$$F_D(t) = \frac{1}{2}\rho \overline{U}^2 B\, C_D(\alpha); \quad F_L(t) = \frac{1}{2}\rho \overline{U}^2 B\, C_L(\alpha) \text{ and } M(t) = \frac{1}{2}\rho \overline{U}^2 B^2\, C_M(\alpha) \tag{1}$$

where C_D, C_L and C_M are respectively the mean drag, lift and moment coefficients determined through wind tunnel tests on small scale sectional models, ρ is air density, U is the mean wind velocity, B is the bridge deck width and α is the mean angle of attack under wind action.

Buffeting forces per unit span of the bridge deck are expressed according to the linearized quasi-steady theory since for the turbulence intensities typical of synoptic winds and for the turbulence components within the practical frequency range the force coefficients may be considered as frequency independent and fluctuating forces as linear functions of fluctuating velocities [6]:

$$F_D(t) = \frac{1}{2}\rho \overline{U}^2 B\left[C_D(\alpha) 2\frac{u(t)}{\overline{U}} + \left(\frac{\partial C_D}{\partial \alpha} - C_L \right) \frac{w}{\overline{U}} \right] \tag{2a}$$

$$F_L(t) = \frac{1}{2}\rho \overline{U}^2 B\left[2C_L \frac{u(t)}{\overline{U}} + \left(\frac{\partial C_L}{\partial \alpha} + C_D \right) \frac{w(t)}{\overline{U}} \right] \tag{2b}$$

$$M(t) = \frac{1}{2}\rho \overline{U}^2 B^2\left[2C_M(\alpha) \frac{u(t)}{\overline{U}} + \frac{\partial C_M}{\partial \alpha}(\alpha) \frac{w\ (t)}{\overline{U}} \right] \tag{2c}$$

where $u(t)$ and $w(t)$ are the fluctuating velocities respectively in the along- wind and vertical directions, and the force coefficients and their derivatives are to be taken at an angle of attack corresponding to the mean wind loading acting on the bridge.

Self-excited forces resulting from the bridge deck motion are usually expressed as functions of the so-called flutter derivatives as formulated by Scanlan [6], which depend on the external shape of the deck and can be determined through wind-tunnel tests of sectional small scale models. Considering the three force components resulting from the motions in lateral, vertical and torsional directions in terms of displacements, velocities and accelerations, the complete formulation include 18 derivatives, H_i*, P_i*, and A_i*, i=1,6. Classic flutter analysis is characterized by the coupling of vertical (y) and torsional (θ) vibrations while torsional flutter is a negative aerodynamic damping stability phenomenon. For the buffeting vibration analysis focused herein all the cross terms in the self-excited forces expressions (for example, vertical force resulting from torsional movement) are neglected since the wind velocities considered are much lower than the critical wind velocity for the flutter onset. Also neglected are the terms associated to inertial forces. The self-excited lift and moment forces are then expressed as:

$$F_L = \frac{1}{2}\rho\overline{U}^2 B\left[KH_1^*\frac{\dot{y}}{\overline{U}} + K^2 H_4^*\frac{y}{B}\right] \qquad \text{and} \qquad M = \frac{1}{2}\rho\overline{U}^2 B^2\left[KA_2^*B\dot{\theta}/\overline{U} + K^2 A_3^*\theta\right] \tag{3}$$

where K is the reduced frequency parameter (=$B\omega/U$). Applying these force components to motion equations in generalized coordinates and transferring them to the left hand side of the equations yield to changes in damping and stiffness characteristics of each vibration mode including vertical and/or torsional movements. Total damping ratio associated to a mode vibration is then written as the sum of the structural and the aerodynamic damping ratios:

$$\bar{\xi} = \xi\frac{\omega}{\overline{\omega}} + \xi_{aer} = \xi\frac{\omega}{\overline{\omega}} - \frac{\rho B^2}{4}\left[B^2 A_2^* G_{\theta\theta} + H_1^* G_{pp} + P_1^* G_{yy}\right] \tag{4}$$

where $G_{\theta\theta}$, G_{pp} and G_{yy} are the modal summations [6].

Theoretical analyses were performed in time domain by solving motion equations in generalized coordinates. Random generation of partially correlated wind fluctuating velocities allowed for the calculation of the aerodynamic forces acting on the towers and on the deck, the latter according to eqs. 2. Turbulence characteristics in the along-wind direction were described by Harris spectral density function while in lateral and vertical directions corresponding functions by Kaimal were used [7]. The components *u*, *v* and *w* of the fluctuating velocity were considered as uncorrelated. As several studies have reported [8], the coherence of buffeting forces is stronger than that of the turbulence fluctuations in the oncoming, undisturbed air flow. Therefore, two cases were considered in the present analyses: total correlation and partial correlation of the forces equal to that of the fluctuating velocities, with decay constants C_y and C_z taken equal to 6 and 10 for the along wind component and equal to 8 and 10 for the vertical one.

3 DESCRIPTION OF THE SMALL SCALE MODELS

Brief descriptions of the small geometric scale topographical model and of both sectional and tridimensional structural models are given in the following.

3.1 Topographical model

Figure 5 shows an aerial view of the bridge site and the printed highway path crossing the Laranjeira Channel, linking the city of Laguna to Pescaria Brava in Santa Catarina state. In this figure, the location of the recently constructed Laguna cable-stayed bridge is marked in red.

Figures 6 and 7 show respectively the 1:2000 scale topographical model inside the wind tunnel [5] and the wind directions for which measurements of fluctuating velocities were taken at 20 level points along vertical lines passing by the center of the bridges main span and by the axis of towers. Measurements were made with hotwire anemometers and used to draw the vertical profiles of normalized mean wind velocity and of the along wind turbulence intensity. Figures 8 (a,b) and 9 (a,b) show these profiles for two wind directions, 354° and 174°, respectively; directions that are almost perpendicular to the tangent to bridge deck axis at the middle section of the central span.

These vertical profiles of mean wind velocity and turbulence intensity shown in Figures 8 and 9 together with all the other profiles related to each angle of wind incidence were simulated in the wind tunnel tests of the 3D aeroelastic model of the complete cable stayed bridge.

The normalized average wind velocity at level *z* is defined as

$$U_{ad}(z) = \overline{U}(z)/\overline{U}_{ref} \tag{5}$$

where $\overline{U}(z)$ is the mean wind velocity and $\overline{U}_{ref}$ is the reference value of the mean wind velocity.

The intensity of turbulence at level *z* is defined as

$$I_u(z) = \sigma_u(z)/\overline{U}(z) \tag{6}$$

where $\sigma_u(z)$ is the standard deviation of the along wind fluctuating velocity.

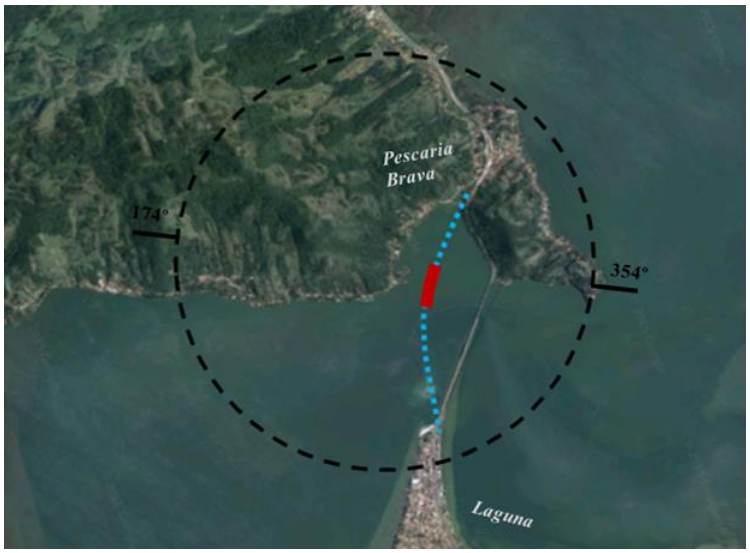

Figure 5. Aerial view of the bridge site; the location of the recently constructed Laguna cable-stayed bridge is marked in red.

Figure 6. Topographical model inside the wind tunnel (scale 1:2000) [5].

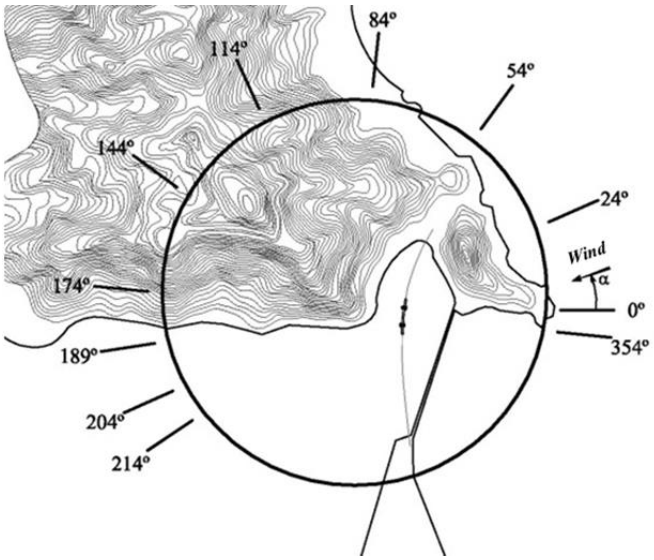

Figure 7. Wind directions on topographic model tests.

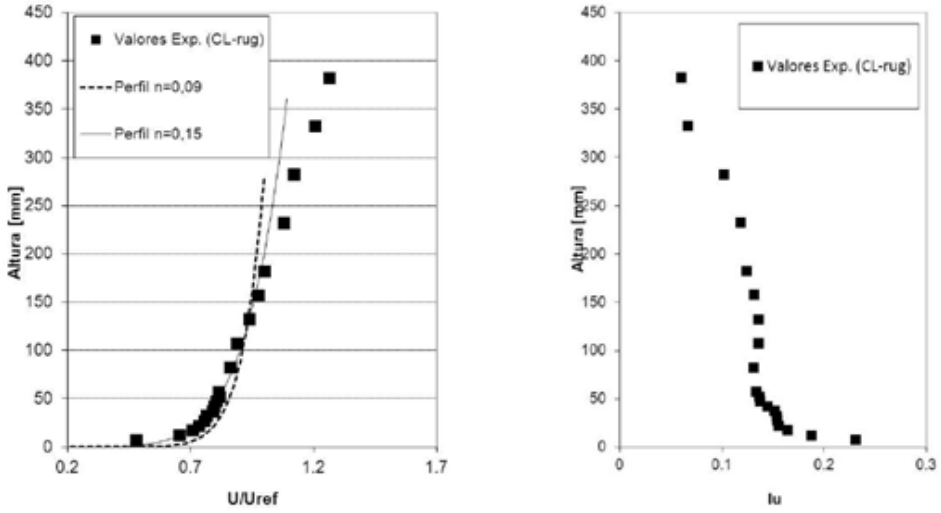

(a) (b)

Figures 8. (a) Normalized average wind velocity vertical profile and (b) Along wind turbulence intensity vertical profile for wind direction equal to 354°.

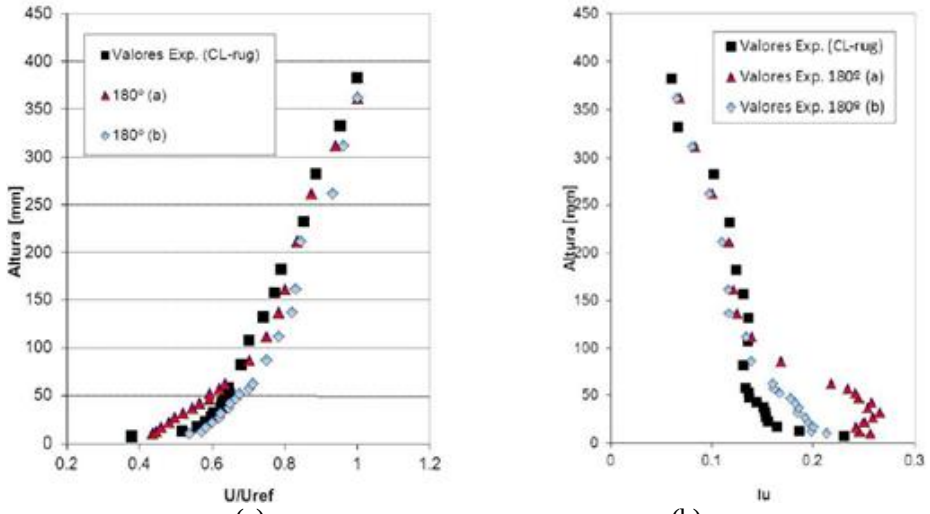

(a) (b)

Figures 9. (a) Normalized average wind velocity vertical profile and (b) Along wind turbulence intensity vertical profile for wind direction equal to 174° [5].

3.2 Brief description of the 3D physical aeroelastic model

The aeroelastic physical model simulates, within the framework of the classical similitude theory, the aerodynamic shape of the structure as well as its dynamic structural behavior. Mass, stiffness and damping properties are represented in the adopted scale of similitude by means of well-established experimental techniques applied in the fabrication of the physical model.

In the present case-example it was adopted a 1:200 length scale resulting in a ~2.0 meters long bridge model. A density scale 1:1 and an acceleration scale 1:1 were adopted, implying that the Froude number is fulfilled and the gravity forces are well represented in order to achieve the correct tensioning of the stay-cables in the reduced scale model of the bridge. This modeling criterion implies that the stiffening scale has to be sought for every structural component of the bridge model. In general this is not an easy task and the always expected small deviations are compensated by adjusting the air flow velocity scale to interpret the wind tunnel test measurements.

Figure 10 shows the ~2.0 meters long 1:200 geometric scale aeroelastic model of the complete cable-stayed bridge inside the wind tunnel [4] Figure 11 illustrates the 3D model instrumented with micro-accelerometers located at various points along the deck and at the top of each tower. Measurements of acceleration x time were taken in the directions given in Table 1, according to the reference axes indicated in Figure 11.

Figure 12 shows some of the component parts of the bridge model deck, foundation blocks and towers, fabricated from aluminum alloy plates, to comply with both mass distribution properties and the bending (vertical and transversal) and torsional stiffness of the deck and lateral bending (in x and y directions) of the towers. The stiffness properties of the deck model were achieved by means of an U-shape aluminum profile carefully machine cut, while the towers stiffness properties were modelled with a narrow flat bar of aluminum. These stiffening elements were encased by complementary elements to model the cross-

sections geometries of the deck and towers and consequent aerodynamic form of each bridge model structural component. The lateral stiffness of the foundations given by the piles into the soil strata were modeled by means of hard steel wires in a number equal to the number of piles for each foundation block. The stay-cables were modeled by means of steel wires and helical springs to achieve the proper axial stiffness and tension. The aerodynamic drag in each stay-cable was modeled by means of discrete bullets (having scaled masses) distributed along their length.

A complete and detailed description of the fabrication and modeling of the small scale bridge structure and its foundations is given in the wind tunnel technical report [4].

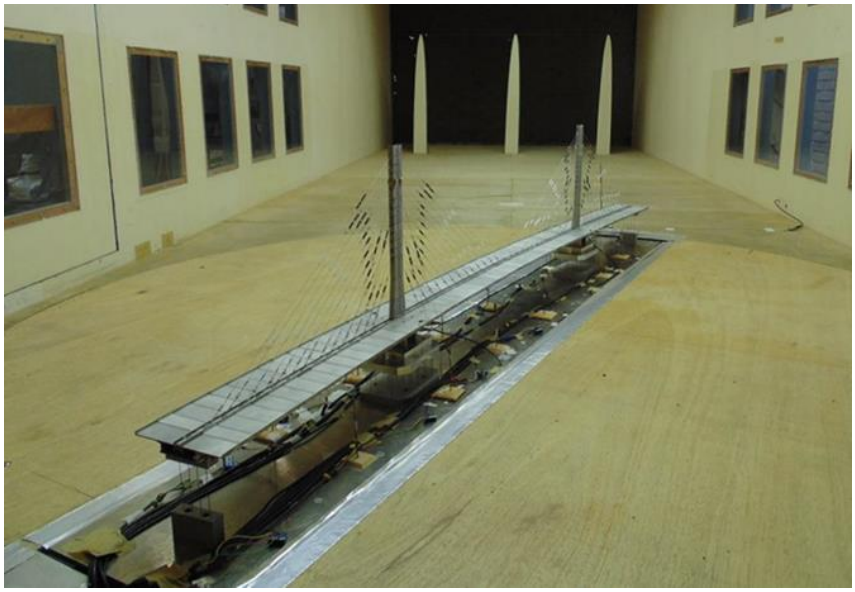

Figure 10. Aeroelastic model of the complete cable-stayed bridge inside the wind tunnel [4].

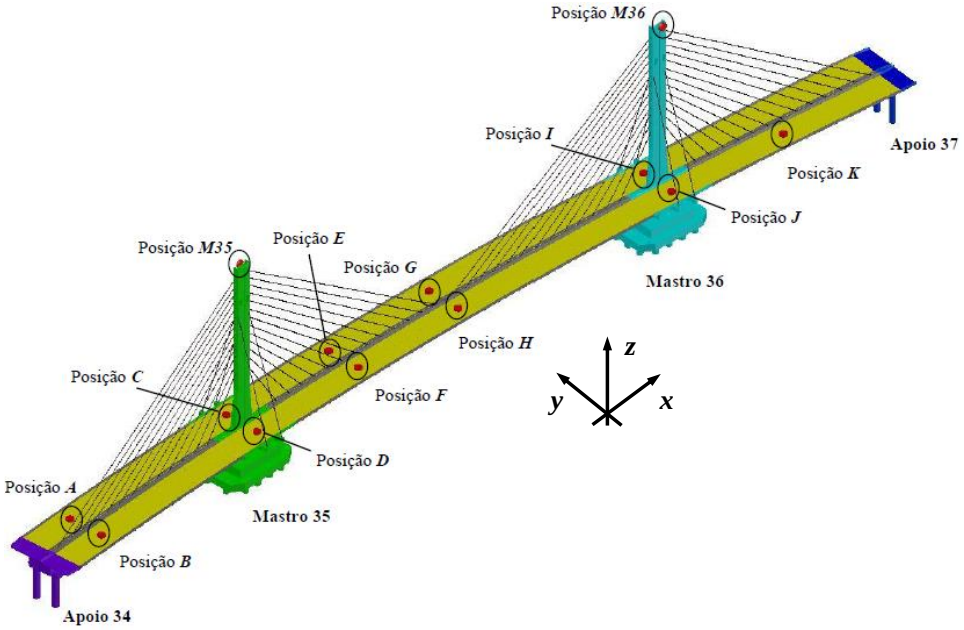

Figure 11. Location of the micro-accelerometers on 3D model (positions A to K, M35 and M36) [4].

Table 1. Points and directions of the acceleration measurements.

Measurement points	A	B	C	D	E	F	G	H	I	J	K	M35	M36
Direction x			X	X					X	X			
y	X	X	X	X	X	X	X	X	X	X	X	X	X
z	X	X			X	X	X	X			X		

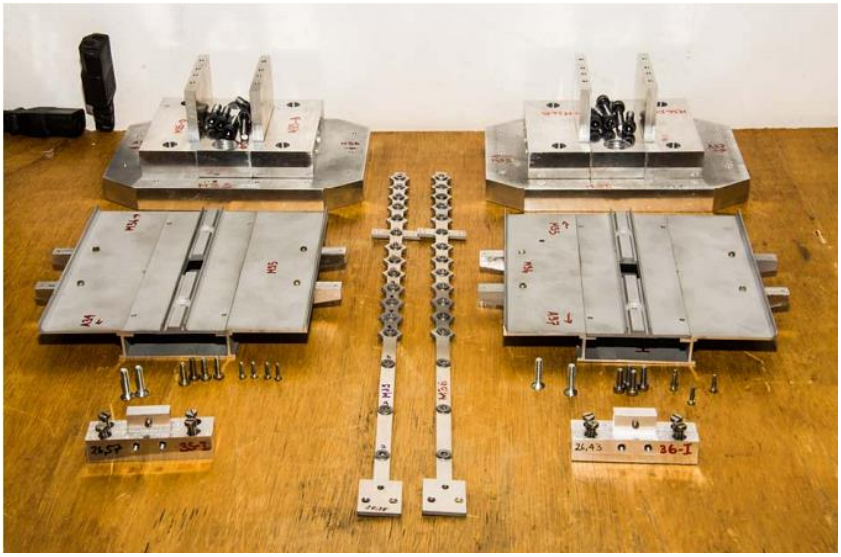

Figure 12. Component parts of the bridge model deck, foundation blocks and towers [4].

3.3 Brief description of the sectional model and results

Because of the geometric complexity of the deck structure of the focused bridge and consequent complexity of the air flow and of the aerodynamic pressures distribution around the deck's cross-section, no simplified approach for the assessment of the bridge's aeroelastic behavior can be applied. Hence, an experimental evaluation of the average aerodynamic forces acting on a stretch of the bridge deck has to be made by means of wind tunnel tests of a reduced scale sectional model.

For the present case-example a length scale1:65 was chosen to construct the sectional model having 1205mm of length which corresponds to a stretch of 78.325 meters of length of the prototype bridge deck. The model was fabricated by composing some distinct materials (aluminum, plastic, ABS and wood) to simulate all the geometric details of the deck structure and its appendages, as for example the NJ barriers (see Fig. 2).

 # Aerodynamic Forces and Coefficients

The sectional model shown in Figure 13 was tested under turbulent (I_u=11%) and smooth (I_u =0,4%) wind flows. The drag and lift forces and torsion moment were determined by measurements (taken with 3-axes load-cells) of the aerodynamic force resultants on the sectional model. A complete description of the mounting and the use of the load-cells is given in the wind tunnel technical reports [9].

The aerodynamic forces acting on the rigid sectional model (kept still during testing) were measured for angles of attack varying between -10º and +10º in steps of 1º according to the signal convention shown in Figure 2; and limited to the given range of degree for the topographical conditions of the focused bridge's site.

Figures 14 present the variation of the aerodynamic coefficients (for this bridge deck) with the angle of attack for turbulent wind flow.

Figure 13. Sectional model inside the wind tunnel [9].

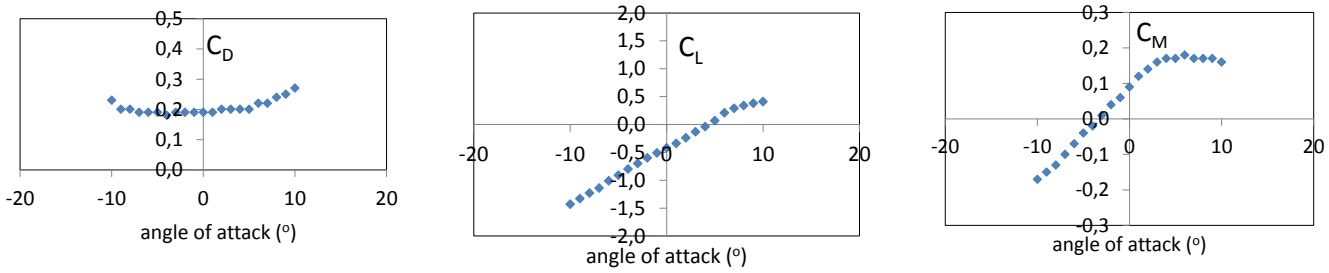

(a) (b) (c)

Figures 14. Drag, lift and moment coefficients for turbulent flow (adapted from [9]).

 # Aerodynamic Damping and Coefficients

The total aeroelastic modal damping ratios are given by the sum of the structural damping (resulting from the addition of the hysteretic or material damping plus the viscous damping of the moving structure immersed in air) and the aerodynamic damping related to the dissipative aeroelastic forces.

The aerodynamic modal damping ratio (see eq. 4) can be estimated by making use of the aeroelastic coefficients (H_1*, P_1*and A_2*), which are determined by means of wind tunnel tests on the same small scale sectional model used to get the aerodynamic coefficients, but now set in motion under both smooth and turbulent flows.

In the tests to determine the aerodynamic coefficients the sectional model is fixed to the 3-axes load-cells in both ends of the model [10]. Now, in the tests to estimate the aeroelastic coefficients the sectional model is connected in both ends to pairs of upper and lower elastic springs attached to a rigid transverse beam, as shown in Figure 15.

The springs have the right stiffness and distance between them which together with the sectional model mass and mass moment of inertia yield vibration frequencies related to the model vertical and angular motions, according to the similitude frequencies scale $k_f = k_L^{-1/2}$. Damping factors associated with the model vertical motion (vertical bending mode of the 3D structure) and angular rotation (torsion mode of the structure) may be provided by dash-pots attached to the ends of the transverse beams. Damping factors should be the same in the model and in the prototype structure, as they are π numbers in the similitude theory.

Among the aeroelastic coefficients (also called aerodynamic derivatives) the most important is the coefficient A_2* which is particularly related to the aeroelastic stability of slender bridge decks. Estimation of A_2*as a function of increasing wind velocity as shown in Figure 16 is made to fulfill the following basic purposes: (i) estimation of the critical wind velocity for torsional aeroelastic instability (flutter); (ii) estimative of the aerodynamic damping as a function of the wind velocity. It should be observed that the critical wind velocity associated with vortex shedding induced vibration in the vertical bending mode (vertical motion of the sectional model) can be directly obtained by monitoring the model dynamic response in terms of amplitudes of vertical motion of the sectional model. The variation with increasing velocity of the peak amplitude of the steady state responses in vertical motion of the model, for two different damping factors is fundamental to obtain the vortex-induced vibration response of the 3D aeroelastic model by means of a simplified modal theoretical approach [6].

However, for the present bridge case-example the results obtained with the sectional model tests in the wind tunnel have demonstrated that both aeroelastic phenomena (flutter and vortex-induced vibration) can only occur for very high wind velocities above the recorded natural wind velocities in the bridge site.

Figure 15. Spring supports of the sectional model [10]

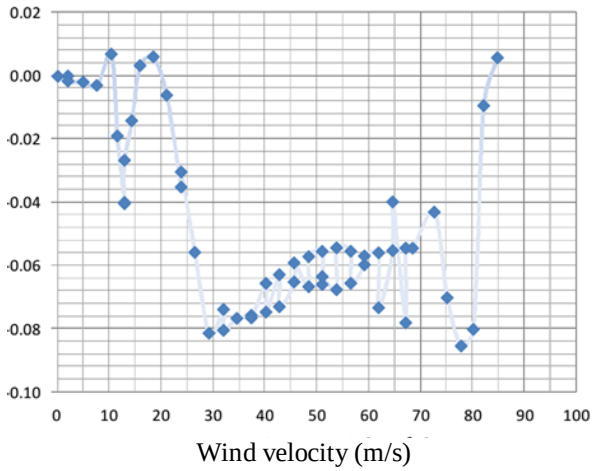

Figure 16. Aerodynamic derivative A_2* as a function of prototype scale wind velocity [11]

4 CORRELATIONS BETWEEN THEORETICAL AND PHYSICAL MODELS DYNAMIC RESPONSES

This section is mainly addressed to the validation of the previously described 3D aeroelastic mathematical – computational modeling of a cable-stayed bridge, which for short is herein called theoretical modeling. This is done by investigating their main dynamic properties and the displayed behavior, and also by correlating the theoretical amplitudes of accelerations at characteristic points and directions with their experimental counterparts obtained from wind tunnel tests on the physical small scale 3D aeroelastic model. The use of maximum values of the acceleration amplitudes or peak values estimated by means of rms values as correlation parameters has a major reason: acceleration signals recorded during wind tunnel tests are raw data not contaminated by inherent errors of any numerical double integration algorithm to get displacements. For the purpose of this validation procedure the used experimental data refer to the E2 case of wind characteristics as described in Section 2 in relation to the wind direction 374^o and mean wind velocity equal to 23.29m/s at 10m height.

4.1 Correlation between modal vibration properties

Table 2 presents a correlation between the first 10 vibration frequencies and mode shapes obtained with the theoretical and physical models. In relation to the description of the vibration mode shapes given in Table 2 it should be explained that mode shape identification from the physical model dynamic response was done by comparing directly stretches of acceleration x time signals taken by sensors located at different points but in the same direction (see Table 1). For example the vertical acceleration x time signal recorded in G and H positions in the physical model (see Fig. 11) were directly compared to detect the vertical bending and torsion coupled mode of dynamic response and their corresponding vibration frequencies were determined by applying the FFT algorithm. Nevertheless it should be also pointed out that because the instrumentation of the model was not made as extensive as needed to this sort of mode shape identification procedure, this work step although successful was not an easy and quick task for the modes related to the bridge model deck. The easiest task was done for the modes dominated by the fundamental lateral bending mode of the towers. The experimental dynamic responses refer to low velocity wind action so that frequencies are not significantly altered by wind-structure interaction.

Table 2. Comparison between theoretical and experimental vibrations frequencies and compound mode shapes.

Mode	Physical model frequency (Hz)	Theoretical model frequency (Hz)	Mode shape of the deck	+	Mode shape of the towers
1	0.44	0.43	anti-symmetric lateral bending		antisymmetric lateral bending
2	0.45	0.47	lateral bending and torsion		symmetric lateral bending
3	0.54	0.52	lateral bending		antisymmetric lateral bending
4	0.64	0.55	longitudinal translation and vertical bending		longitudinal bending
5	0.69	0.57	vertical and lateral bending		symmetric lateral bending
6	0.87	0.60	vertical bending and torsion		longitudinal and lateral bending
7	Not observed	0.72	lateral bending		antisymmetric lateral bending
8	0.91	0.92	lateral bending		symmetric lateral bending
9	0.97	0.99	vertical bending		still
10	1.12	1.17	symmetric vertical bending		still

In relation to the correlation between theoretical and experimental frequencies one can note that: (i) compound modes dominated by the towers´ fundamental lateral bending mode have well correlated frequencies; (ii) conversely the coupled

vertical and torsion mode of the deck is not well correlated. The reason for this seems to be due to rotational stiffness of the foundation blocks and piles simulated in the small scale model. This view is supported by the fact that this stiffness property was not verified in the fabrication and mounting of this block-piles assemblage, but its lateral bending stiffness property which is essential to simulate transversal bending of the deck coupled with the lateral bending of the towers.

4.2 Damping properties

Damping ratios for groups of compound modes constitute π numbers in the similitude theory and therefore should be the same in the reduced model and in the prototype. Usual damping ratios which have been measured in main structural components of existing cable-stayed bridges and used in the design stages of the structure are very difficult to be reproduced in a small scale 3D physical model.

However, for the only purpose of validation of the theoretical model this fact can be disregarded as one can take in it the damping ratios extracted from the physical model itself. For this it should be observed that damping in the complex system of a cable-stayed bridge and its foundations is not of a viscous equivalent Rayleigh type, i.e proportional to the modal mass and stiffness overall properties. Instead damping ratios are associated with the bridge´s main structural components (namely towers and deck) or more truly with groups of vibration modes associated with the dominant modes of these components.

Table 3 presents the damping ratios estimated by means of the logarithm decrement technique applied to the free vibration responses of the reduced model subjected to impacts at the tip of the towers and at the middle section of the central span deck.

Table 3. Damping ratios associated to the towers and deck.

Component / point location	Vibration frequency (Hz)	Damping ratio (%)
Deck / G	0.866	5.10
Tower / M35	0.446	0.84
Tower / M36	0.455	0.80

4.3 Correlation between acceleration amplitudes

Table 4 presents a correlation between theoretical and experimental results in terms of acceleration amplitudes in three characteristic points of the bridge structure: vertical acceleration at the middle section of the central span and lateral acceleration at the tip of the two towers. For each one of the two models (physical and theoretical) it is given for each point: (i) the maximum value of the acceleration amplitude found in the acceleration x time response over a 600 seconds time interval; (ii) the *rms* values of these responses; (iii) the peak values obtained with the expression

$$a_{peak} = g\sigma_a \; ; \qquad g = \sqrt{2\ln(\nu T)} + \frac{0.577}{\sqrt{2\ln(\nu T)}} \tag{7}$$

where σ is the standard deviation, in this case the *rms* value, *g* is the peak factor and νT is the number of zero up crossings for the considered 600s response.

What can be noted promptly is the very favorable correlations found between the theoretical and the experimental results, as shown in the last two columns of Table 4. This impressively good correlation was found by considering in the theoretical model a total correlation of the fluctuating aerodynamic forces acting on the bridge deck and a partial correlation of these forces along the height of the towers. The reason for taking this approach is mainly because no span wise measurement of fluctuating velocities was made across the width of the wind tunnel at the level of the bridge deck, while measurements of fluctuating velocities were made along several vertical lines during the wind tunnel tests of the topographic model (see Section 3.1).To investigate the effect of a partial correlation of fluctuating aerodynamic forces acting on the bridge deck new dynamic responses were obtained with the theoretical model (see Section 2). Correlation of results for peak values of acceleration are presented in Table 5 where it can be observed that the referred effect is not so large and results are still favorably well correlated, as shown in the last two columns of Table 5.

Table 4. Theoretical and experimental acceleration amplitudes (m/s^2)

Measurement points and directions	Physical model in wind-tunnel			Theoretical - computational			Ratio Theoretical/physical	
see Fig. 11	max	peak	*rms*	max	peak	*rms*	max	peak
G-H Direction z	0.312	0.331	0.076	0.333	0.358	0.086	1.07	1.08
G-H Direction y	0.154	0.169	0.041	0.144	0.171	0.041	0.93	1.01
M35 Direction y	0.623	0.707	0.151	0.642	0.707	0.171	1.03	1.00
M36 Direction y	0.649	0.870	0.185	0.646	0.760	0.169	1.00	1.14

Figures 17 and 18 are shown to demonstrate the favorable correlation between experimental (Fig. 17) and theoretical (Fig. 18) time responses and frequency spectra for the lateral acceleration response at the tip of one tower (point M36 in Fig.11).

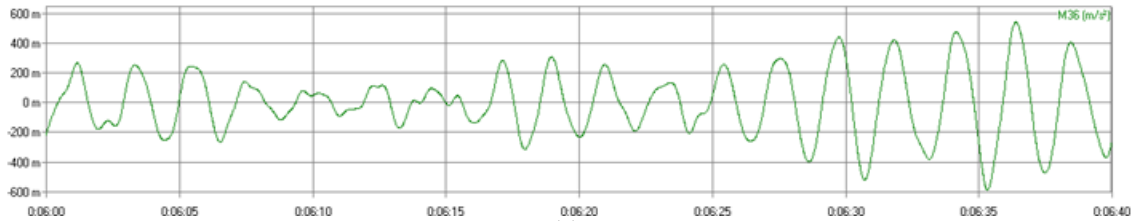

(a)

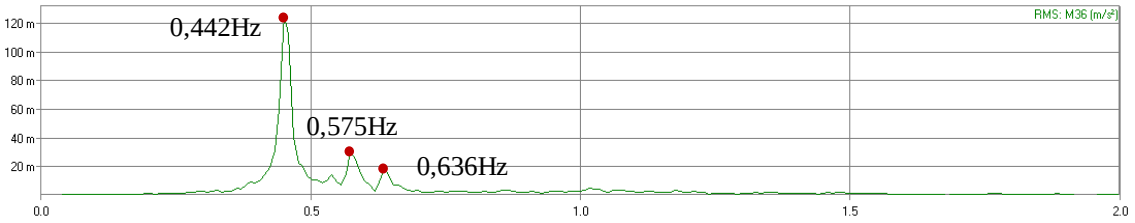

(b)

Figures 17. Experimental lateral acceleration response at the tip (M36 in Fig.11) of the tower (a) time stretch of the acceleration signal; (b) frequency spectrum.

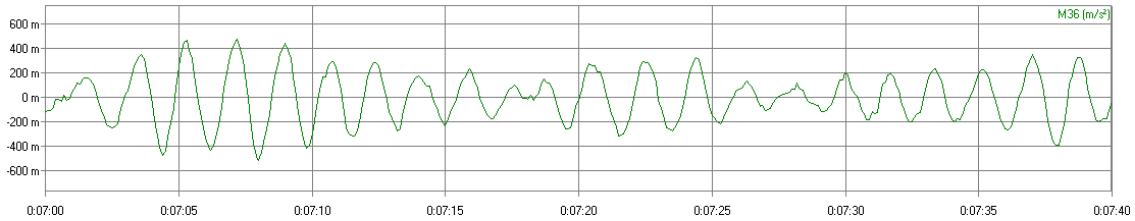

(a)

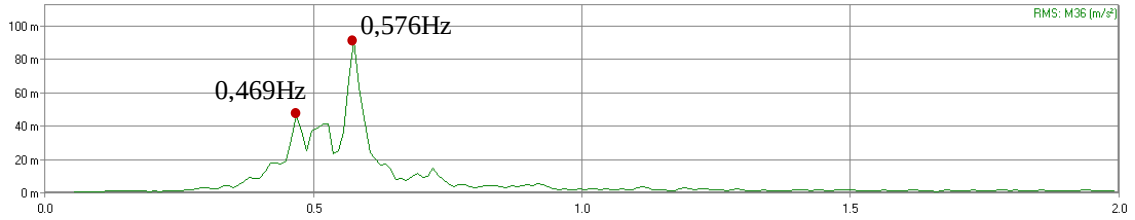

(b)

Figures 18. Theoretical lateral acceleration response at the tip (M36 in Fig.11) of the tower (a) time stretch of the acceleration signal; (b) frequency spectrum.

Table 5. Theoretical and experimental peak acceleration amplitudes (m/s^2). TC = total correlation; PC=partial correlation

Measurement points and directions (see Fig. 11)	Physical model in wind-tunnel	Theoretical – computational TC	Ratio Theoretical TC / physical	Theoretical – computational PC	Ratio Theoretical PC / physical
Middle central span G-H Direction z	0.331	0.358	1.08	0.369	1.12
Middle central span G-H Direction y	0.169	0.171	1.01	0.162	0.96
Top of tower M35Direction y	0.707	0.707	1.00	0.744	1.05
Top of tower M36 Direction y	0.870	0.760	0.87	0.683	0.79

5 RESULTS FOR DESIGN PARAMETERS

Considering that the local wind characteristics (i.e. vertical profiles of the variation of mean velocity and intensity of turbulence) were not available at the design stage for performing adequate aeroelastic analysis of a cable-stayed bridge, the design engineers have to resort to technical recommendations found in design codes and in the classical literature.

Within this scenario the recommendations given by the Brazilian design code NBR-6123/1988 in relation to the terrain roughness Category I are taken to model the aerodynamic forces acting on the bridge structure for wind direction equal to 354^o (see Figs. 7 and 8). According to the experimental damping data related to bridge structure found in the technical literature [1,13] the following values were taken for the damping ratios of groups of compound vibration modes associated with bending of the towers (ξ_{towers} = 2.0%) and with the bending of the deck (ξ_{deck} = 4.0%).

Table 6 presents a comparison between theoretical results obtained for two distinct scenarios: (A) the same scenario for which the theoretical model yielded the results presented at the last but one column of Table 5; (B) the new scenario for which the Brazilian Code recommendations are taken into account together with the given damping ratios, and for which partial correlations of the fluctuating aerodynamic forces are also considered. To demonstrate the great influence of the chosen damping ratios on the aeroelastic response it is also included in Table 6 numerical results (between parenthesis) referred to the same wind characteristics taken from scenario A but for distinct values of damping ratios (ξ_{towers} = 2.0%; ξ_{deck} = 4.0% instead of ξ_{towers} = 0.8%; ξ_{deck} = 5.0%). It can be seen that the peak responses associated to lateral bending (direction y) significantly decreased thanks to the greater damping value ξ_{towers}. Even the vertical response of the deck decreased indicating that the towers motion dominates the overall response. Comparing the values related to lateral bending in Scenario B to those between brackets in Scenario A it can be concluded that the wind velocity characteristics along the upper portion of the towers are similar in both scenarios. Conversely, the vertical response (direction z) at the middle of the central span increased due to the greater values of the mean wind velocity and turbulence intensity at the deck height in Scenario B. At the deck level the mean velocity and the turbulence intensities related to Scenario B are respectively 23% and 15% greater than in Scenario A. Therefore the aerodynamic fluctuating forces are around 40% greater in Scenario B.

Table 6. Comparison between theoretical peak accelerations (m/s²) for two distinct sets of wind and damping characteristics.

Measurement points and directions (see Fig. 11)	Theoretical – computational – PC (see Table 5) Scenario A	Theoretical – computational – PC (with design parameters) Scenario B	Ratio Theoretical B / Theoretical A
Middle central span G-H Direction z	0.369 (0.351)	0.495	1.34 (1.41)
Middle central span G-H Direction y	0.162 (0.135)	0.127	0.78 (0.94)
Top of tower M35Direction y	0.744 (0.482)	0.496	0.67 (1.03)
Top of tower M36 Direction y	0.683 (0.504)	0.552	0.81 (1.09)

Table 7 presents the total displacement amplitudes (mean + peak fluctuating) at the same points given in Table 6 for acceleration amplitudes and for the same two scenarios A and B. These figures follow the same trends shown for acceleration amplitudes.

Table 7. Comparison between theoretical displacements (cm) for two distinct sets of wind and damping characteristics.

Measurement points and directions (see Fig. 11)	Theoretical – computational – PC (see Table 5) Scenario A	Theoretical – computational – PC (with design parameters) Scenario B	Ratio Theoretical B / Theoretical A
Middle central span G-H Direction z	2.87	4.41	1.54
Middle central span G-H Direction y	1.87	1.35	0.72
Top of tower M35Direction y	11.3	6.45	0.57
Top of tower M36 Direction y	10.4	6.74	0.65

Regarding the internal forces in the structural components Table 8 presents results the most loaded stay-cable and Table 9 presents results for the lateral bending moments at the base section of the towers. It is seen that these critical internal forces in Scenario B resulted ~25% greater than in Scenario A. It should be observed that internal force values calculated for the design scenario B in all others structural components resulted 10% to 26% greater than in Scenario A.

Table 8. Comparison between theoretical tension forces (kN) in one typical stay-cable for two distinct sets of wind and damping characteristics.

Stay-cable	Theoretical – computational – PC (see Table 5) Scenario A	Theoretical – computational – PC (with design parameters) Scenario B	Ratio Theoretical B / Theoretical A
Most loaded stay-cable	238	295	1.24

Table 9. Comparison between lateral bending moments (kNm) at towers base for two distinct sets of wind and damping characteristics.

Tower	Theoretical – computational – PC (see Table 5) Scenario A	Theoretical – computational – PC (with design parameters) Scenario B	Ratio Theoretical B / Theoretical A
A (M35) M_x	20709	26093	1.26
B (M36) M_x	18773	23621	1.26

6 CONCLUDING REMARKS

Some relevant remarks on the art of modeling 3D aeroelastic behavior of cable-stayed bridges may be drawn from the correlation between theoretical and experimental results and comparisons of theoretical results for distinct scenarios of wind characteristics and design parameters. These are the following.

In relation to the design parameters modal damping ratios are the most relevant as they can only be determined from measurements on existing structures and therefore should be continuously collected to help in the structural design of new bridges.

The 3D theoretical-computational aeroelastic models of those structures - which make use of aerodynamic and aeroelastic coefficients taken from wind tunnel tests on sectional models - are well appropriated to develop optimum structural design for very long and slender cable-stayed bridges and present several practical advantages over the 3D physical aeroelastic model whenever this requires very large wind tunnel facilities.

Carefully designed and constructed small scale 3D physical model of not so long bridges (down to the 1:200 geometrical scale) that fits in ordinary tunnel facilities can be used to study the aeroelastic behavior and to validate the 3D theoretical model with which an optimum structural design can be developed.

Recommendations of the design codes may lead to either conservative or non conservative values of the aerodynamic forces and consequent response amplitudes depending on the topographic aspects of the bridge site.

The last remark is that topographical models of the bridge site are essential to describe the wind flow characteristics to be used in both theoretical and physical 3D aeroelastic models and in this way overcoming some difficulties found when applying design codes recommendations. Topographical models are in this sense essential for physical modeling in any size of wind-tunnel facilities.

REFERENCES

[1] Fujino Y; Kimura K; Tanaka H. Wind Resistant Design of Bridges in Japan – developments and Practice, Springer, 2012.

[2] Lobo Carneiro F. Dimensional analysis and theory of similitude of physical models (in Portuguese). Editora da UFRJ, Rio de Janeiro, 1993.

[3] Sedov, L.; Similitude et Dimensions en Mécanique, Editions Mir, Moscow, 1977.

[4] Vento-S and LAC/UFRGS; Wind Tunnel Technical Report – Wind tunnel tests of 3D complete aeroelastic model of the cable-stayed bridge over the Canal Laranjeiras - BR-101 – Laguna – SC (in Portuguese), April 2015.

[5] Vento-S and LAC/UFRGS; Wind Tunnel Technical Report – Estimation of topographic effects on oncoming flow at the cable-stayed bridge over the Canal Laranjeiras site (in Portuguese), March 2015.

[6] E. Simiu and R. Scanlan, Wind Effects on Structures: an introduction to wind engineering. John Wiley & Sons, New York, USA, 1986.

[7] J. Blessmann, Introduction to the Study of Dynamic Wind Action (in Portuguese), Editora da Universidade - UFRGS, Porto Alegre, Brazil, second edition, 2005

[8] C. Dyrbye and S. O. Hansen, Wind Loads on Structures, John Wiley & Sons, New York, USA, 1997.

[9] Vento-S and LAC/UFRGS; Wind Tunnel Technical Report – Deck mean aerodynamic coefficients of the cable-stayed bridge over the Canal Laranjeiras - BR-101 – Laguna – SC (in Portuguese), September 2014.

[10] Vento-S and LAC/UFRGS; Wind Tunnel Technical Report – Critical wind velocities for flutter and vibration induced by vortex-shedding of the cable-stayed bridge over the Canal Laranjeiras - BR-101 – Laguna – SC (in Portuguese), October 2014.

[11] Vento-S and LAC/UFRGS; Wind Tunnel Technical Report – Aerodynamic derivative A2 of the deck section of the cable-stayed bridge over the Canal Laranjeiras - BR-101 – Laguna – SC (in Portuguese), September 2014.

[12] ABNT - Associação Brasileira de Normas Técnicas. Norma Brasileira NBR-6123 (NB-599): Forças Devidas ao Vento em Edificações, Rio de Janeiro, Brazil, 1988.

[13] Narita, N.; Yokoyama, K.; A summarized account of damping capacity and measures against wind action in cable-stayed bridges in Japan, in Cable-stayed Bridges - Recent Developments and their Future - Proceedings of the Seminar, Elsevier, Japan, 10-11 December 1991.